

## Molecular Mimics of Insulin-like Growth Factor 1 (IGF-1) for Inhibiting IGF-1: IGF-Binding Protein Interactions

Henry B. Lowman,<sup>\*,‡</sup> Yvonne M. Chen,<sup>‡</sup> Nicholas J. Skelton,<sup>‡</sup> Deborah L. Mortensen,<sup>§</sup> Elizabeth E. Tomlinson,<sup>§</sup> Michael D. Sadick,<sup>||</sup> Iain C. A. F. Robinson,<sup>⊥</sup> and Ross G. Clark<sup>#</sup>

*Departments of Protein Engineering, Endocrinology, and BioAnalytical Technology, Genentech, Inc., South San Francisco, California 94080, Division of Neurophysiology, National Institute for Medical Research, London, U.K., and Research Centre for Developmental Medicine and Biology, School of Medicine, University of Auckland, Auckland, New Zealand*

*Received February 23, 1998; Revised Manuscript Received April 21, 1998*

**ABSTRACT:** IGF-1 (insulin-like growth factor 1) is a 70-residue protein hormone which has both metabolic and mitogenic activities mediated through IGF-1 binding to cell surface receptors. However, an unrelated class of proteins, the IGF-binding proteins (IGFBPs) also bind IGF-1 in the serum and tissues and block or modulate its activity in vivo. Therefore, inhibitors of the IGFBPs can alter the distribution between free and bound IGF-1 [Loddick, S. A., Liu, X.-J., Lu, Z.-X., Liu, C., Behan, D. P., Chalmers, D. C., Foster, A. C., Vale, W. W., Ling, N., and De Souza, E. B. (1998) *Proc. Natl. Acad. Sci. U.S.A.* 95, 1894–1898] and potentially affect the distribution of IGF-1 among body tissues. We report here that phage-displayed peptide libraries have yielded a peptide that binds IGFBP-1 and produces IGF-like activity at sub-micromolar concentrations. The 14-residue peptide has an extremely well-defined solution conformation that can aid in the design of smaller, orally active compounds. Interestingly, the peptide structure contains a helix, as does one region of IGF-1 previously implicated in IGFBP binding, yet displays side chains different from those of the IGF-1 helix I. Furthermore, an IGF-1 variant lacking receptor-signaling activity in vitro is shown here to produce IGF-like mitogenic and metabolic activity in vivo. These results suggest that small antagonist mimetics of protein ligands, identified by binding selection to otherwise inhibitory factors, may be useful as indirect agonists for a variety of therapeutic applications.

The multiple activities of the insulin-like growth factors (IGFs<sup>1</sup>), extending from hypoglycemia to whole body growth, have led to IGF-1 being used as an injectable drug in tests as a therapeutic for several human diseases (reviewed in refs 1–3). The type I IGF receptor mediates the activities of IGF-1 and is similar in structure to the insulin receptor (4, 5). Orally active compounds that have similar effects could be therapeutically useful in treating a variety of potential indications, including short stature, renal failure, and type I or type II diabetes (2). However, discovering small molecule agonists for these receptors has proved difficult (6). In general, a direct agonist mimic of IGF-1

must both bind to the receptor and induce a complex activation event (4). Further complicating this approach from a drug-design viewpoint, IGF-1 appears to undergo a conformational change in binding to its receptor (7, 8).

In vivo, the IGFs are bound to a family of binding proteins (IGFBPs), unrelated to the IGF-1 receptor, which modulate IGF activity (reviewed in refs 9 and 10). Six distinct IGFBPs are known in humans (9), and other related proteins have been described. Binding of some IGFBPs to IGF-1 effectively blocks the action of IGF-1. In fact, the vast majority of IGF-1 present in serum circulates as a complex with one binding protein, IGFBP-3, and a third protein, ALS (11). The remaining binding proteins form lower-molecular weight complexes with IGF-1, some of which are localized to cell surfaces in a tissue-specific manner (9).

IGF-1 has been shown to have a diffuse epitope for binding to its binding proteins, including residues near the N terminus as well as residues 49–51 (12–14). Nevertheless, it has been shown that the epitope on IGF-1 used to bind its receptors is different and distinct from the one used to bind IGFBPs. For example, mutating two tyrosines in a recombinant human (rh) IGF-1, Y24L/Y29A IGF-1, produces a molecule that is still able to bind to IGFBPs but binds very poorly to IGF receptors (15–17), showing that the structural requirements for receptor binding and IGFBP binding may be completely unrelated.

Molecules that bind to IGFBPs might potentiate some of the effects of IGF-1, by liberating IGF-1 from binding protein

\* Corresponding author. Telephone: (650) 225-1171. Fax: (650) 225-3734. E-mail: hbl@gene.com.

<sup>‡</sup> Department of Protein Engineering, Genentech, Inc.

<sup>§</sup> Department of Endocrinology, Genentech, Inc.

<sup>||</sup> Department of BioAnalytical Technology, Genentech, Inc.

<sup>⊥</sup> National Institute for Medical Research.

<sup>#</sup> University of Auckland.

<sup>1</sup> Abbreviations: ALS, acid-labile subunit of the IGF-1 ternary complex; BSA, bovine serum albumin; COSY, two-dimensional correlated spectroscopy; 2QF-COSY, double-quantum filtered COSY; EPO, erythropoietin; g8p, major coat protein of bacteriophage M13; hGH, human growth hormone; IGF-1, insulin-like growth factor 1; IGFBP-1, IGF binding protein 1; iv, intravenous; ip, intraperitoneal; NNS, degenerate codon with nucleotides N (A, G, C, or T) and S (G or C); NOE, nuclear Overhauser effect; NOESY, two-dimensional NOE spectroscopy; rhIGF-1, recombinant human IGF-1; rh Y24L/Y29A IGF-1, rhIGF-1 with mutation of Tyr24 to Leu and Tyr29 to Ala; sc, subcutaneous; rms, root-mean-squared; ROESY, rotating frame Overhauser effect spectroscopy; TOCSY, total coherence spectroscopy.

complexes either in the serum or at tissue-specific sites in the body. Hence, antagonism of a protein–protein binding event could potentially be used to produce net agonist activity. Indeed, Loddick et al. (18) have recently shown IGF-like neuroprotective activity in rat brain using a “receptor-inactive” IGF-1 variant. Some of the binding proteins, on the other hand, have the ability to potentiate IGF-1 action (reviewed in refs 9 and 10). IGFBPs may exert IGF-independent effects, including interactions with tissue-specific components which act to target IGF-1 to these tissues as IGF–IGFBP complexes (9). In this case, blocking the binding of IGF-1 specifically could reduce its effects in tissues where attenuation of mitogenesis is desired (19).

As a model for indirect agonist drug design, we chose IGFBP-1 as a target. Using phage-displayed peptide libraries, we have identified novel peptides, unrelated to IGF-1 in sequence, which bind to IGFBP-1 and can free IGF-1 from IGFBP-1-bound complexes in vitro. Surprisingly, one such peptide, identified from a phage-displayed peptide library, also has a well-defined turn–helix structure in aqueous solution, suggesting the possibility of designing small molecule mimetics. To test for multiple IGF-like effects of an indirect agonist in vivo, we needed a high-affinity IGFBP inhibitor with the ability to bind IGFBPs in an animal model system. The IGF-1 variant Y24L/Y29A IGF-1 was therefore chosen as a molecule having IGFBP-binding activity but lacking in vitro receptor binding. The results of these experiments suggest that novel IGF-1 mimetics can be found for binding IGFBPs and that blocking IGFBP binding to IGF-1 can have IGF-like mitogenic and metabolic effects in vivo.

## EXPERIMENTAL PROCEDURES

**Construction of Peptide–Phage Libraries.** A peptide–g8p fusion (20) was constructed for polyvalent display of peptide on filamentous phage. The gene for the major coat protein (g8p) of *Escherichia coli* bacteriophage M13 was amplified from M13K07 (Stratagene) using PCR primers 5′-GCA CGC TTC TAG AAC GGT GGC GGT GCT GAG GGT GAC GAT CCC GCA and 5′-AGT AGC TCT AGA CAC TGA GTT TCG TCA CCA GTA CAA AC. The *Xba*I-digested fragment was used to replace the g3 fragment of phGHam-g3 (21) to construct a g8p display phagemid. The hGH gene of this plasmid was replaced with cDNA for an antibody-recognizable (gD tag) peptide to produce a fusion product containing the gD peptide (in italics), followed by a linker peptide (underlined), and the g8p of *E. coli* bacteriophage M13, SGTAMADPNRFRGKDLAGSPGGGSGG-GAEGDDPAKAAFNLSLQASATEYIGYAWAM-VVVIVGATIGIKLFFKFTSKAS.

Several random-sequence peptide libraries were constructed using single-stranded template-directed mutagenesis (22), with the form  $X_jCX_kCX_k$  (where  $j$  ranged from 4 to 10 and  $i + j + k = 18$ ), using oligonucleotides of the form 5′-GCT ACA AAT GCC TAT GCA (NNS)<sub>i</sub> TGC (NNS)<sub>j</sub> TGC (NNS)<sub>k</sub> GGT GGA GGA TCC GGA GGA G-3′. These libraries yielded  $5.3 \times 10^8$ ,  $5.6 \times 10^8$ ,  $5.0 \times 10^8$ ,  $6.3 \times 10^8$ ,  $4.5 \times 10^8$ ,  $1.9 \times 10^8$ , and  $2.1 \times 10^8$  *E. coli* transformants, respectively, for  $j = 4–10$ . An unconstrained peptide library, of the form  $X_{20}$ , yielded  $5.0 \times 10^8$  transformants. Additional libraries were constructed with the form

SGTACX<sub>2</sub>GPX<sub>4</sub>CSLAGSP or X<sub>4</sub>CX<sub>2</sub>GPX<sub>4</sub>CX<sub>4</sub>, yielding  $1.8 \times 10^8$  and  $7.9 \times 10^8$  transformants, respectively.

**Peptide–Phage Binding Selections for IGFBP-1.** IGF-BP-1 was biotinylated with EZ-Link NHS-SS-biotin (Pierce). Immunosorbant plates (Nunc Maxisorp) were coated with 2 μg/mL Neutravidin (Pierce) in 50 mM sodium carbonate buffer (pH 9.6) and blocked with BSA (5 g/L in carbonate buffer). After incubation for 1 h with biotinylated IGFBP-1 (20 nM), plates were washed with 0.05% Tween 20 in PBS buffer. Phage from the libraries described above were pooled as follows. Pool A consisted of SGTACX<sub>2</sub>GPX<sub>4</sub>CSLAGSP phage, pool B of X<sub>4</sub>CX<sub>2</sub>GPX<sub>4</sub>CX<sub>4</sub> phage, pool C of X<sub>20</sub> phage, and pool D of combined phage from the X<sub>j</sub>CX<sub>j</sub>CX<sub>k</sub> ( $j = 4–10$ ) libraries. The initial selection was carried out by binding phage, washing, and then eluting by incubation with 50 mM DTT (to reduce the biotin–disulfide linkage, releasing phagemid particles) for 1 h at room temperature. Phage were propagated overnight with shaking at 37 °C in XL1-Blue cells with M13-VCS or M13-K07 helper phage (Stratagene).

In the second and third cycles of binding selection, streptavidin (0.1 mg/mL, Pierce) was included in the phage cocktails along with biotin, and 5 g/L ovalbumin, or 5 g/L instant milk in 50 mM sodium carbonate buffer, was used as the blocking agent. The fourth round was carried out on plates directly coated with 2 μg/mL IGFBP-1 or with albumin only. Phage remaining bound were eluted by incubating with 20 mM HCl, after which the eluates were neutralized with 1/5 volume of 1 M Tris-HCl (pH 8.0). Propagation was carried out as above.

**Peptide Synthesis.** Peptides were synthesized by either manual or automated (Milligen 9050) Fmoc-based solid-phase synthesis on a 0.25 mmol scale using a PEG–polystyrene resin (23). Upon completion of synthesis, side chain protection groups were removed and the peptide was cleaved from the resin with 95% trifluoroacetic acid (TFA) and 5% triisopropylsilane. Oxidation of the disulfide bonds was carried out by adding a saturated iodine solution in acetic acid. Purification of peptides was performed by reversed-phase HPLC with a water/acetonitrile gradient containing 0.1% TFA. The purity of each peptide was determined by analytical HPLC to be greater than 95% homogeneous, and its identity was verified by mass spectrometry.

**Peptide Inhibition of IGF Binding to IGFBP-1 by ELISA.** For inhibition of IGFBP-1 binding, IGFBP-1 (as well as IGFBP-3 as a control) was biotinylated as described above. Immunosorbant plates were coated and blocked as above, using 2 μg/mL IGF-1. In a separate plate, serial dilutions of peptide were premixed with a constant concentration (20 nM) of biotinylated IGFBP-1. After 20 min at room temperature, the mixture was added to the IGF-1 plate. The peptide/IGFBP mix was then removed, and the plate was washed with PBS buffer containing 0.05% Tween 20. Bound biotin–IGFBP-1 was detected using streptavidin-conjugated horseradish peroxidase and a chromogenic substrate (*o*-phenylenediamine, Sigma) with product detection at 492 nm. In some experiments, the tetramethylbenzidine substrate (Kirkegaard and Perry, Gaithersburg, MD) was used, with product detection at 450 nm.

**Cell-Based KIRA Assay of IGF-1 Activity.** A kinase receptor activation assay (KIRA) for measuring activation of the human type 1 IGF-I receptor was developed using

human MCF-7 cells (ATCC-HTB 22), which express IGF receptors as well as insulin receptors (24). Cells were grown overnight in 96-well plates with medium (50:50 F12/DMEM, Gibco) at 37 °C in 5% CO<sub>2</sub>. Supernatants were decanted, and stimulation media (50:50 F12/DMEM with 25 mM HEPES and 2.0% BSA) containing either experimental samples (IGFBP-1, preincubated for 30 min with peptide and then for 30 min with 50 ng/mL rhIGF-1) or the rh IGF-I standards were added. After stimulation at 37 °C for 15 min, supernatants were decanted, and cells were lysed. Lysates were transferred to an immunosorbant plate coated with the polyclonal anti-IGF-IR (Santa Cruz Biotech) and blocked with BSA. After incubation for 2 h at room temperature, unbound receptor was removed by washing, and bound receptor was detected with biotinylated antibody 4G10 (anti-phosphotyrosine) followed by development with HRP-conjugated dextran–streptavidin and tetramethylbenzidine substrate solution. The product absorbance at 450 nm was read with a reference at 650 nm.

**NMR Spectroscopy.** NMR data were collected with a Bruker AMX-500 spectrometer at 30 °C and pH 5.3 and a peptide concentration of 6.7 mM. Spectra were processed and analyzed using the program Felix [Molecular Simulations Inc. (MSI), San Diego, CA]. 2QF-COSY, TOCSY, ROESY, and NOESY data were collected from a H<sub>2</sub>O solution as described (25), except that excitation sculpting was used for solvent suppression (26). NOESY, ROESY, and COSY-35 spectra were acquired from a D<sub>2</sub>O solution. Sequential resonance assignments were made by standard methods (27) and are presented in the Supporting Information (Table S1). <sup>1</sup>H–<sup>1</sup>H distance and dihedral angle restraints were obtained from the ROESY and COSY data, respectively, as described previously (28). Eighty structures were calculated using the programs DGII (29) and the amber force field implemented within DISCOVER (MSI) using 149 distance restraints, 10  $\phi$  restraints, and 5  $\chi^1$  restraints, applied with force constants of 25 kcal Å<sup>-2</sup> or 100 kcal rad<sup>-2</sup>; explicit hydrogen bond restraints were not employed. The 20 structures with the lowest residual restraint violation energy ( $0.22 \pm 0.06$  kcal mol<sup>-1</sup>) were used to represent the solution structure of p1-01; a detailed analysis of the quality of the ensemble can be found in the Supporting Information (Table S2). The final structures have mean maximum distances or dihedral violations of  $0.06 \pm 0.01$  Å or  $0.8 \pm 0.2^\circ$ , respectively. When the three partially disordered N-terminal residues and C-terminal glycine are discounted, the mean rms displacement from the mean structure is  $0.33 \pm 0.10$  and  $0.76 \pm 0.10$  Å for backbone and all heavy atoms, respectively.

**Injection of the IGF-1 Variant in Rats.** All experimental procedures and study designs involving animals were approved by the Genentech Animal Care and Use Committee. Sterile instruments and aseptic technique were used throughout. Animals used were normal Sprague-Dawley rats (SD; 200–240 g/each) (Charles River, Hollister, CA), Zucker diabetic fatty rats (ZDF; 240–280 g/each) (Genetic Models, Indianapolis, IN), hypophysectomized rats (Taconic Farms, Germantown, NY), or homozygous dwarf rats (dw/dw) (30; Charles River).

For injections, the ventral and dorsal neck areas of rats were shaved and prepared with betadine and alcohol. A small skin incision was made ventrally in the neck over the jugular vein. The vein was isolated and a catheter (Mi-

crorenathane tubing) was inserted. The catheter was then led subcutaneously (sc) behind the ears so that it could exit in the dorsal-scapular region for experimental purposes. Incisions were closed with 3-0 silk in a simple continuous fashion. The animals were then allowed to recover on a heated pad and were returned to their cage when they were ambulatory.

For minipump delivery of the IGF-1 variant, rats were anesthetized using ketamine (65 mg/kg) or xylazine (12.5 mg/kg) intraperitoneally (ip). The skin over the dorsal-scapular implantation site was surgically clipped and prepared using betadine and alcohol. A 1 cm incision was made in the skin, and two Alza 2001 osmotic minipumps were placed sc before the site was closed with 9 mm staples. The animals were allowed to recover on a heated pad and were returned to their cages when they were ambulatory.

Rat IGF-1 levels were measured using an RIA (Diagnostic Systems Labs, Webster, TX) as described by the manufacturer. This assay is specific for rat (endogenous) IGF-1 and measures total IGF-1 (including that bound to IGFBPs). Insulin values were measured using an RIA (Linco Research, St. Charles, MO). Serum creatinine and glucose levels were determined on a Chem 1A serum chemistry analyzer (Bayer Corp., Pittsburgh, PA). For determination of organ weights, animals were sacrificed after 7 days.

## RESULTS

**IGFBP-1-Specific Ligands from Phage-Displayed Libraries.** To test whether molecular mimics smaller than IGF-1 could be found to bind specifically to the IGFBPs, peptide–phage libraries (31) were screened for peptides that could bind to purified human IGFBP-1 and block its interaction with IGF-1. While simple, structurally unconstrained peptide–phage libraries have sometimes yielded peptides that bind to specific protein targets (reviewed in ref 32), introduction of a single disulfide bond joining Cys residues within a short peptide often favors ligands which bind their targets with higher affinities than unconstrained forms (see, e.g., refs 33 and 34). We therefore constructed peptide–phage libraries with potential disulfide bonds in the form X<sub>i</sub>CX<sub>j</sub>–CX<sub>k</sub>, where  $i = 4–7$ ,  $j = 4–20$ , and  $k = 4–7$ , to favor small, structurally compact peptide ligands. The libraries used a polyvalent phage presentation to access a wide range of binding affinities through avidity effects (35–38). In addition, some libraries contained a fixed Gly-Pro sequence, to favor a type 1 reverse turn (reviewed in ref 39), as observed previously in the bound hairpin conformation of a peptide agonist of the erythropoietin (EPO) receptor (40, 41). In particular, two such libraries contained the fixed CX<sub>2</sub>–GPX<sub>4</sub>C motif, found in the EPO–agonist peptide, with either fixed (SGTACX<sub>2</sub>GPX<sub>4</sub>CSLAGSP) or random (X<sub>4</sub>CX<sub>2</sub>GPX<sub>4</sub>–CX<sub>4</sub>) flanking residues.

When these phage libraries were affinity-sorted on the basis of binding to IGFBP-1, enrichments (ratio of phage eluting from IGFBP-1-coated plates to phage eluting from control plates) of 10–1000-fold were observed in selection cycles 3 and 4 for three libraries: library A (GP motif with fixed flanking residues), B (GP motif with random flanking residues), and C (combined CX<sub>j</sub>C motifs, where  $j = 4–10$ ). No significant enrichment was observed from library D (linear X<sub>20</sub> library). Several predominant sequences were

Table 1: Peptide Sequences of g8-Phagemid Clones Binding to IGFBP-1

name	sequence <sup>a</sup>	pool	frequency
Φ1	SEVGC <u>R</u> AGPLQWLCEKYF	A	6/6
Φ1	SEVGC <u>R</u> AGPLQWLCEKYF	B	5/6
Φ13	KDPVC <u>G</u> EGPLMRICERLF	B	1/6
Φ31	EVDGRWWIVETFLAKWDHMA	C	6/6

<sup>a</sup> Underlined residues were invariant in the designed libraries. Peptide sequences were deduced from the DNA sequences of clones obtained after four rounds of binding selection from pools A–C. The frequency represents the occurrence of each clone among the total number of clones sequenced from the indicated pool.

identified which bound specifically to IGFBP-1, and their displayed peptides were deduced from DNA sequencing (Table 1). Binding of these peptide–phage to immobilized IGFBP-1 was blocked by IGF-1, and little or no peptide–phage binding was detected on immobilized IGFBP-3 (data not shown). Two of the peptide sequences, Φ1 and Φ13, contained the fixed Gly-Pro motif within a 10-residue disulfide loop; the third, Φ31, contained no Cys residues or Gly-Pro motif. On the basis of DNA sequencing, the occurrence of Φ1 in pool A (Table 1) likely represents a cross-contamination event from library B, followed by efficient selection for the clone over authentic members of library A.

**Functional Characterization of Synthetic Peptides.** Peptides were prepared by chemical synthesis to correspond to the phage-derived sequences. To test for IGFBP-1 binding, we preincubated each peptide with biotinylated IGFBP-1 and measured residual binding to IGF-1 in a plate-based (ELISA) assay. Peptides CRAGPLQWLCEKYFG (p1-01, cyclic) and SEVGCRA<sup>1</sup>GPLQWLCEKYFG (p1-02, cyclic), both based upon the predominant phage clone Φ1 (Table 1), showed the highest affinities for IGFBP-1, blocking IGFBP-1 binding to IGF-1 with IC<sub>50</sub>s of 180 and 50 nM, respectively (Figure 1A). The peptide p3-01, namely SEEVCWPVAEWYLCN-MWG (cyclic), was identified by a phage-displayed library screen similar to that described for IGFBP-1, using biotinylated IGFBP-3 as the target (H. B. Lowman et al., in preparation). This peptide did not effectively block the binding of IGFBP-1 to IGF-1 (Figure 1A). Furthermore, the binding of p1-01 and p1-02 was quite specific for IGFBP-1. Although IGF-1 blocked biotinylated IGFBP-3 binding to immobilized IGF-1, the IGFBP-1-selected peptides did not (Figure 1B). In contrast, peptides p1-13 and p1-31, corresponding to phage clones Φ13 and Φ31, respectively (Table 1), bound IGFBP-1 much more weakly, blocking IGF-1 binding with IC<sub>50</sub>s of 5.4 and >10 μM, respectively (data not shown).

A cell-based *in vitro* kinase activity (KIRA) assay was also used to test the effects of p1-01 and p1-02 peptides on cells having functional IGF receptors in cell culture. In this assay, cells stimulated with IGF-1 show increased levels of phosphorylated receptors (24), with an EC<sub>50</sub> of about 1.7 nM IGF-1 (not shown). In this case, the results show that, whereas IGFBP-1 blocks IGF-1-dependent kinase activity, both peptides liberate IGF-1 activity from mixtures containing IGFBP-1 (Figure 2A). The EC<sub>50</sub>s (400 nM for p1-01 and 190 nM for p1-02), while higher than those in the plate assay, reflect a similar relative decrease in potency for the shorter synthetic peptide compared to that for the full-length

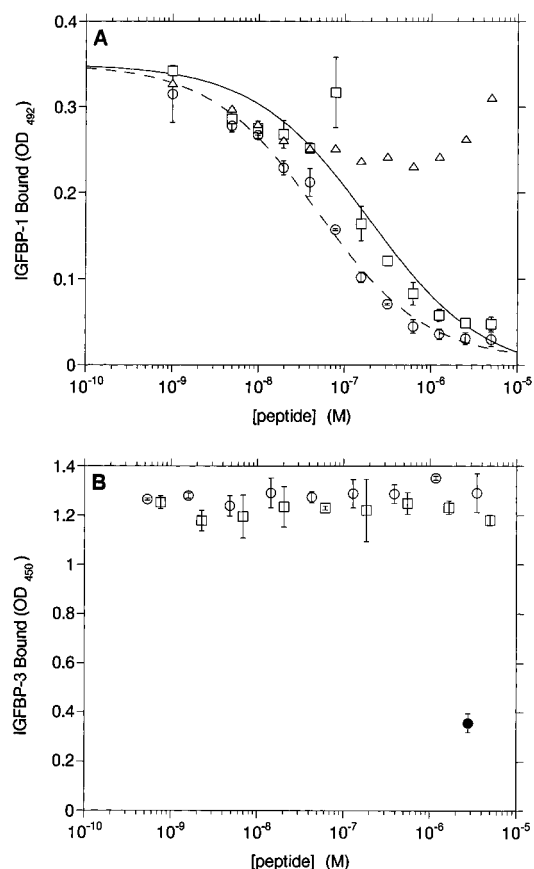


FIGURE 1: Peptide inhibition of IGFBP-1 binding to IGF-1. (A) Peptides p1-01 (□) and p1-02 (○) were preincubated with IGFBP-1 before the mixtures were added to an IGF-1-coated plate, as was a control peptide selected for binding IGFBP-3, p3-01 (△). (B) Peptides p1-01 (□) and p1-02 (○), both of which were selected for binding IGFBP-1, were preincubated with IGFBP-3 and the mixtures added to an IGF-1-coated plate. An IGF-1 control (●) is also shown.

peptide. In contrast to the IGFBP-1-selected peptides, the IGFBP-3 selectant p3-01 did not liberate IGF-1 activity from IGF-1–IGFBP-1 mixtures (Figure 2A). The peptides themselves exhibited no direct agonist activity (data not shown), nor did they inhibit IGF-1 activity (Figure 2B).

**Structural Characterization of the p1-01 Peptide.** <sup>1</sup>H NMR was used to evaluate the structure of the p1-01 peptide in solution. Chemical shifts, scalar coupling constants, and nuclear Overhauser enhancements all indicate that the peptide adopts a well-defined and stable conformation in aqueous solution, even at 30 °C (see Experimental Procedures and the Supporting Information). Restraints based on the NMR data were used to calculate an ensemble of structures for p1-01 using a combination of distance geometry and restrained molecular dynamics calculations. The peptide p1-01 contains a well-defined C-terminal helix encompassing residues Leu6–Tyr13, preceded by a type I reverse turn at Pro5–Leu6 (Figure 3). The helix does not contain a typical N-cap motif, but a hydrogen bond is observed between H<sup>N</sup> of Trp8 and the carbonyl oxygen of Pro5 in 19 of the final 20 structures. The four N-terminal residues are not defined well by the NMR data. The driving force for formation of this structure appears to be hydrophobic packing of residues on one face of the helix; Leu6, Leu9, and Tyr13 form a central stripe, with Trp8, Lys12, and Phe14 packing against these residues.

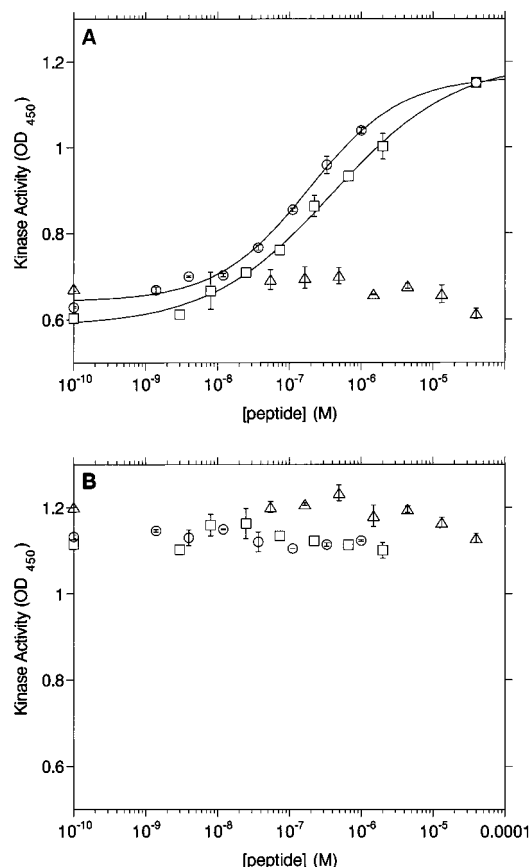


FIGURE 2: Indirect agonist activity of peptides on cells in vitro. A kinase receptor activation assay was used to monitor IGF-1 activity. (A) IGF-1 was mixed with IGFBP-1 and peptides p1-01 (□) or p1-02 (○) or a IGFBP-3 binding peptide, p3-01 (△), and then the mixtures were added to MCF-7 cells. EC<sub>50</sub>s for release of IGF-1 activity were calculated to be 400 nM for p1-01 and 190 nM for p1-02. (B) IGF-1 was mixed with peptides p1-01 (□) or p1-02 (○) or a IGFBP-3 binding peptide, p3-01 (△), and then the mixtures were added to MCF-7 cells.

The disulfide bond is also necessary for structure, presumably in helping to initiate the first turn of the helix. A peptide, SRAGPLQLSEKYFG, with both Cys residues replaced by serine was also studied by NMR. Chemical shifts, scalar coupling constants, and interresidue NOEs were all consistent with an extended or random-coil structure. This peptide showed inhibition of IGFBP-1 binding to IGF-1 with an IC<sub>50</sub> of approximately 50  $\mu$ M (data not shown).

Many resonances of p1-01 are broad at temperatures lower than 20 °C, and several resonances (especially the upfield-shifted methyl signals) have concentration-dependent chemical shifts suggestive of some self-association process. In addition, weak NOEs were observed between side chain protons of Tyr13 and Leu6. These NOEs were not used in the determination of a structure for p1-01 and correspond to interproton distances greater than 8 Å in the structures shown in Figure 3, but might easily be explained if the peptide formed a head-to-tail dimer via the hydrophobic helical face. However, collection of NMR data in the presence of 20% acetonitrile prevented self-association without altering the parameters that are indicative of structure. Also, at micromolar concentrations and below, the peptide was shown to be monomeric by analytical ultracentrifugation (data not shown). Thus, the self-association observed at high concentrations in aqueous solution is not necessary for structural

stability of p1-01 or for binding to IGFBP-1. The large solvent-exposed hydrophobic face along the helix (Figure 3) provides an attractive surface for interaction with IGFBP-1 but may be responsible for self-association of the peptide at the high concentrations required to conduct the NMR analysis.

**Insulin-like Effects of an IGF-1 Variant Lacking Receptor Activity.** An IGF-1 variant, rh Y24L/Y31A IGF-1, lacking receptor-binding activity, but still able to bind to IGFBPs (15–17) was chosen to examine the effect of blocking IGFBPs in vivo. We first confirmed the lack of receptor-mediated activation by the variant, and its ability to bind to IGFBPs. Even at high concentrations, rh Y24L/Y29A IGF-1 was inactive in two in vitro bioassays yet was only 5-fold reduced in binding to IGFBP-1 and IGFBP-3 (data not shown).

To test the IGF-1 variant in vivo, chronically cannulated, nonfasted, conscious, normal SD (Sprague-Dawley) adult rats or obese, male Zucker diabetic fatty (ZDF) rats were given a single intravenous (iv) injection of 100  $\mu$ g of rhIGF-1, rh Y24L/Y31A IGF-1, or excipient. In both rat strains, rhIGF-1 and the IGF variant produced large decreases in plasma insulin (Figure 4A,C). Ten minutes after the injections in ZDF rats (Figure 4A), insulin values were  $8.9 \pm 1.3$  ng/mL for the saline treatment,  $4.8 \pm 0.4$  ng/mL for the rhIGF-1 treatment, and  $5.8 \pm 0.9$  ng/mL for the variant treatment. Glucose values (Figure 4B) were  $170 \pm 7$  mg/dL for saline,  $123 \pm 6$  mg/dL for rhIGF-1, and  $145 \pm 7$  mg/dL for the variant. Responses to both rhIGF-1 and the variant were highly significant compared with responses to saline ( $p < 0.01$  for both). Similar results were obtained in normal rats, although the variant's effect on glucose levels was muted (Figure 4C,D).

**Growth-Promoting Effects of the Receptor-Inactive IGF-1 Variant.** Growth promotion is also an important and potentially useful in vivo effect of IGF-1. Therefore, the long-term growth-promoting effect sc infusions of rh Y24L/Y31A IGF-1 were studied in models of complete or partial growth hormone (GH) deficiency, namely, hypophysectomized (Hx) rats or homozygous dwarf (dw/dw) rats, respectively. Both types of rats are sensitive to the growth-promoting effects of IGF-1 (30). Body growth was evaluated in terms of weight gain, cartilage growth, serum chemistries, and weights of IGF-sensitive organs. In Hx rats, which have lower endogenous IGF-1 levels than dw/dw rats (Table 2), rh Y24L/Y31A IGF-1 (50  $\mu$ g/dL) alone significantly increased epiphyseal plate width (controls of  $191 \pm 5$  vs  $233 \pm 9$   $\mu$ m,  $p < 0.01$ ). It also increased kidney size and lowered serum creatinine levels; when given with rhGH, the variant additively stimulated weight gain and spleen growth. rhGH increased endogenous IGF-1 levels (Table 2), perhaps enhancing the amount of IGF-1 that could be displaced by rh Y24L/Y31A IGF-1. In homozygous dw/dw rats (Table 2), rh Y24L/Y31A IGF-1 had additive effects (particularly on the kidney) when co-infused with rhIGF-1. Furthermore, the variant significantly changed the body weight gain and renal responses to hGH injections. Rat IGF-1 levels were reduced by treatment for 7 days with either rhIGF-1 or Y24L/Y31A rhIGF-1, with their combination producing the largest decrease (Table 2).

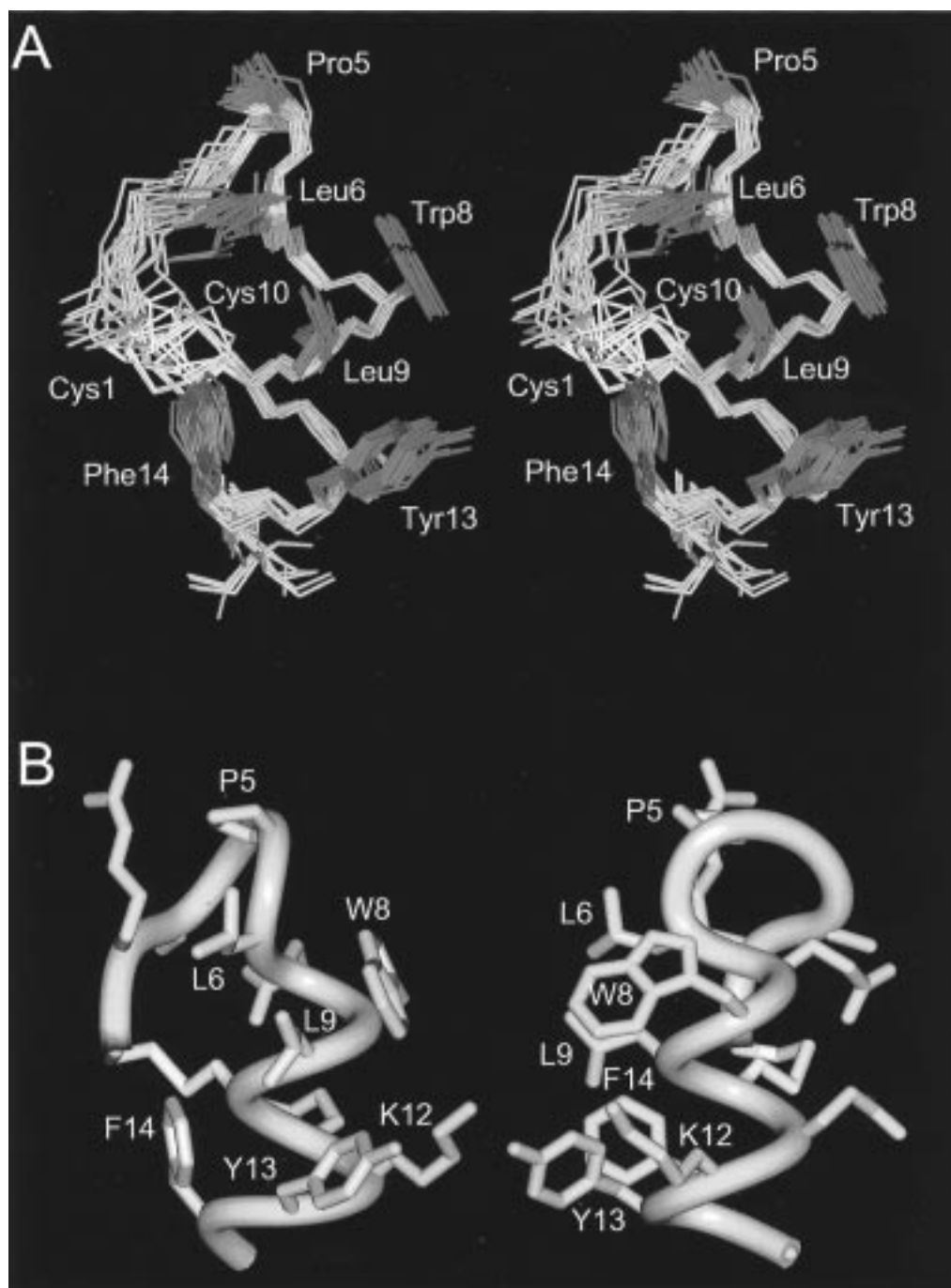


FIGURE 3: Structure of IGFBP-1 binding peptide p1-01. (A) Stereoview of an ensemble of 20 structures of p1-01 determined from NMR data. The backbone is shown in light blue; the cysteine side chains are shown in yellow and several of the other well-defined side chains in darker blue. (B) Ribbon views in two orientations (rotated by 90° with respect to each other) of a representative p1-01 structure showing the hydrophobic packing along one face of the helix. All side chain heavy atoms are depicted. This figure was prepared using the program Insight II (MSI).

## DISCUSSION

*Identification of a Structured IGF-1 Mimic for Binding IGFBP-1.* Simple binding selections using polyvalently displayed peptides on filamentous phage yielded several sequences specific for IGFBP-1. Peptides p1-01 and p1-02 (Table 1), based upon one of these sequences, showed inhibition of IGF-1 binding to IGFBP-1 in the sub-micromolar concentration range (Figure 1). In cell-based assays, the peptides were able to liberate IGF-1 activity from mixtures of IGF-1 with IGFBP-1 (Figure 2). The binding inhibition and the release of IGF-1 activity were both binding

protein-specific, as such effects were not seen with IGFBP-3 (Figures 1 and 2). These properties suggest that IGF-like indirect agonist activity can be induced by a mimetic that binds IGFBPs.

Interestingly, even though no specific selection technique was used to restrict selection to the IGF-1 binding epitope on IGFBP-1, each of the peptides identified from phage-displayed peptide libraries did inhibit the binding of IGFBP-1 to IGF-1. A similar observation was made by Kay et al. (42), who noted that peptide ligands for protein targets from a 38-mer peptide-phage library were most often found for

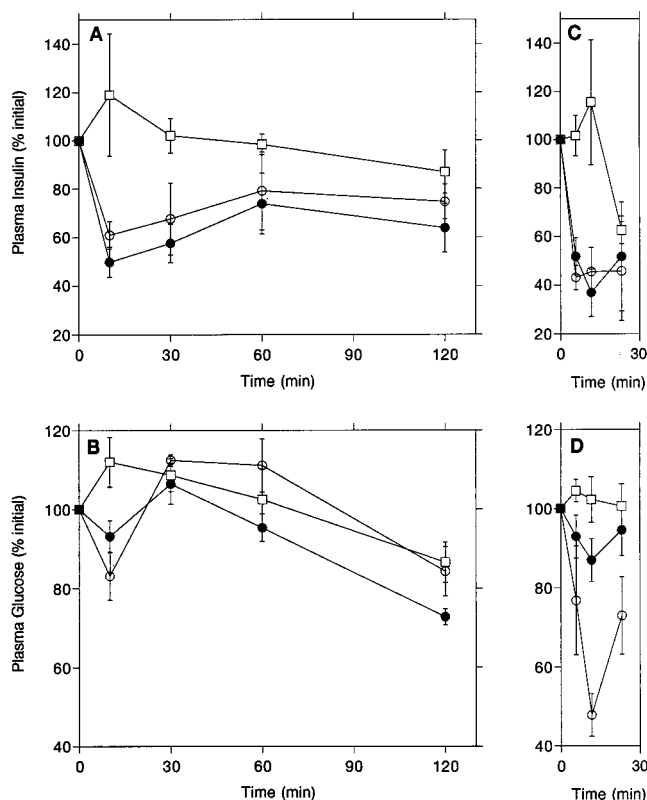


FIGURE 4: Effects of IGF-1 variants on insulin and glucose levels. Chronically cannulated, conscious obese male Zucker diabetic fatty (ZDF) rats (panels A and B) or normal SD rats (panels C and D) were given a single intravenous (iv) injection of 100  $\mu$ g of rhIGF-1 (○), rh Y24L/Y31A IGF-1 (●), or excipient (□). At time points after the injections, insulin values (panels A and C) and glucose levels (panels B and D) are shown as mean  $\pm$  SEM.

targets with known "binding pockets". Although some nonblocking (with respect to ligand–receptor pairs) peptides have also been observed in other systems (see, e.g., ref 43), these results provide support for the notion that peptides from such libraries may often be found to interact with the epitope used in natural protein–protein interactions.

**Structural Implications of the Peptide Mimic.** The p1-01 peptide is, to our knowledge, the most structurally defined peptide in solution yet to be identified from random peptide–phage libraries without a predefined structural scaffold. Although p1-01 does have seven residues in common with the  $\beta$ -hairpin EPO-agonist peptide (40), including the CX<sub>2</sub>GPX<sub>4</sub>C fixed motif, its solution structure (Figure 3) is very different from that of the crystallographically defined EPO-agonist peptide (41) bound to its receptor. A solution structure of the free EPO-agonist peptide has not been reported.

The p1-01 peptide appears to represent a novel structural motif for binding the IGF-1 binding site of IGFBP-1. In a sequence comparison to IGF-1, the p1-01 peptide contains only a short segment, LQWLC<sub>10</sub>, whose sequence is similar to the C-terminal portion of IGF-1 helix 1, LQFVC<sub>18</sub>. Although the backbone and some side chain atoms of these segments can be overlaid reasonably well [rms deviation of N, C $\alpha$ , and C atoms is 0.66 Å between the minimized mean structures from the p1-01 and IGF-1 ensembles (44)], these residues are not thought to interact with IGFBP-1. In IGF-1, mutations of Q15 have little effect on IGFBP-1 binding, mutations of F16 do reduce IGFBP-1 binding but are thought

to do so by destabilizing the native IGF-1 fold, while residues L14, V17, and C18 are all buried and therefore cannot contact IGFBP-1 directly unless the IGF-1 undergoes a very large structural reorganization upon binding (8). Thus, this limited sequence similarity between p1-01 and IGF-1 likely has little functional significance.

In an effort to identify any common structural features between the peptide and IGF-1, residues Pro5–Phe14 of p1-01 were overlaid on all contiguous 10-residue fragments of IGF-1 (44) and mini-IGF-1 (45). Although rms displacement of backbone atoms was low (<1.0 Å) for some of these overlays, there was little or no sequence identity between the peptide and these protein segments. Further, the regions of structural similarity did not encompass those regions of IGF-1 that have been shown by mutagenesis to be important for IGFBP-1 binding, namely, residues at the N terminus and residues 49–51 (12–14). Thus, although IGF-1 and p1-01 share helical regions in their structures, an epitope common to both is not apparent. This conclusion, however, is subject to the caveat that either molecule may change conformation upon binding to IGFBP-1.

A search of the protein database [Dayhoff version 34.233; SwissProt 34 (October 1996); PIR 53 (June 1997)] revealed sequence similarities of 60–75% between p1-02 and short fragments (12–16 residues) of several diverse proteins, including mitochondrial processing peptidase (OCMP1), hepatitis C core protein (HCU21254\_1), and ape leukemia virus receptor (I48084). None of these proteins has obvious structural or functional relevance to IGF-1 or its binding proteins.

The peptides reported here bind IGFBP-1 with much lower affinity than does IGF-1, which has an apparent  $K_d$  of about 1 nM (8). Affinity maturation (see, e.g., refs 21 and 40) using monovalent phage display may yield improved binding affinities for these peptides. Furthermore, an understanding of the specific interactions involved in the binding of peptides with defined structures such as p1-01 should facilitate the design of smaller molecules with improved oral bioavailability by mimicking the binding determinants of such peptides on organic scaffolds. Such molecular mimicry has already been employed using peptide leads to generate small molecule drugs (46), and the development of a systematic means of generating such leads, either through protein minimization (47, 48) or through selection of structured peptides from diversity libraries (41; reviewed in ref 32), should facilitate these efforts.

**A Mechanism for *In Vivo* Activity of a Receptor-Inactive IGF Variant.** *In vivo* experiments show that the IGF-1 variant rh Y24L/Y31A IGF-1 can mimic IGF-1 activity on insulin secretion and blood glucose (Figure 4). Since this variant lacked receptor binding (15–17) and receptor-mediated activity in *in vitro* KIRAs, its action is consistent with an "indirect agonist" effect. Such competition could occur *in vivo* through kinetic trapping of newly synthesized IGFBPs or through mass action, in which IGF-1 first dissociates from IGFBP-bound complexes (Figure 5). Considering the previously reported slow kinetics for dissociation ( $t_{1/2}$  = 1–5 h) of IGF-1 from IGFBP complexes (8, 49), it seems likely that the former mechanism dominates *in vivo*.

**Potential for Therapeutic Development.** The *in vivo* results with growth-deficient rats suggest that rh Y24L/Y31A IGF-1 shows IGF-like growth effects (Table 2) by displacing

Table 2: Responses to Long-Term Exposure to IGF-1 or rh Y24L/Y31A IGF-1 in Rats<sup>a</sup>

treatment	weight gain (g)	[rat IGF-1] (ng/mL)	spleen (% of wt)	kidney (% of wt)	[creatinine] (mg/dL)
Hx group					
excipient	1.5 ± 0.5	56 ± 13	0.19 ± 0.01	0.66 ± 0.02	0.28 ± 0.02
variant	2.7 ± 0.5	30 ± 16	0.21 ± 0.01	0.70 ± 0.02 <sup>b</sup>	0.20 ± 0.04 <sup>b</sup>
GH	18.9 ± 0.6 <sup>b</sup>	536 ± 41 <sup>b</sup>	0.22 ± 0.01	0.67 ± 0.02	0.15 ± 0.03 <sup>b</sup>
GH + variant	22.6 ± 1.4 <sup>b,c</sup>	452 ± 95 <sup>b</sup>	0.27 ± 0.02 <sup>b,c</sup>	0.68 ± 0.03	0.15 ± 0.03 <sup>b</sup>
dw group					
excipient	2.0 ± 1.0	968 ± 175	0.24 ± 0.005	0.79 ± 0.03	0.28 ± 0.02
variant	4.0 ± 0.5	555 ± 42 <sup>b</sup>	0.27 ± 0.009	0.82 ± 0.01	0.23 ± 0.03
IGF	9.3 ± 2.0 <sup>b</sup>	407 ± 63 <sup>b</sup>	0.34 ± 0.012 <sup>b</sup>	0.85 ± 0.03	0.22 ± 0.05
IGF + variant	9.7 ± 0.9 <sup>b</sup>	250 ± 54 <sup>b</sup>	0.37 ± 0.015 <sup>b</sup>	0.92 ± 0.04 <sup>b</sup>	0.18 ± 0.02 <sup>b</sup>
GH	17.2 ± 1.2 <sup>b</sup>	1106 ± 99	0.29 ± 0.01 <sup>b</sup>	0.75 ± 0.01	0.33 ± 0.02
GH + variant	21.3 ± 0.7 <sup>b,c</sup>	857 ± 49 <sup>c</sup>	0.31 ± 0.01 <sup>b,c</sup>	0.79 ± 0.02 <sup>c</sup>	0.25 ± 0.02 <sup>c</sup>

<sup>a</sup> Homozygous dw/dw rats (dw group;  $n = 6$  or  $7$ ) were treated with rhGH (10  $\mu\text{g/dL}$ ), IGF-1 (100  $\mu\text{g/dL}$ ), variant (100  $\mu\text{g/dL}$ ), variant (100  $\mu\text{g/dL}$ ) and IGF-1 (100  $\mu\text{g/dL}$ ), variant (100  $\mu\text{g/dL}$ ) and rhGH (10  $\mu\text{g/dL}$ ), or excipient. Hypophysectomized (Hx group;  $n = 4-6$ ) rats were treated with variant (50  $\mu\text{g/dL}$ ), variant (50  $\mu\text{g/dL}$ ) combined with rhGH (10  $\mu\text{g/dL}$ ), rhGH alone (10  $\mu\text{g/dL}$ ), or excipient. IGF-1 and variant were given by continuous sc minipump; rhGH was given by sc injection (bid). Values are shown as mean  $\pm$  SEM. <sup>b</sup> $p < 0.05$  compared with that of excipient. <sup>c</sup> $p < 0.05$  compared with that of rhGH only.

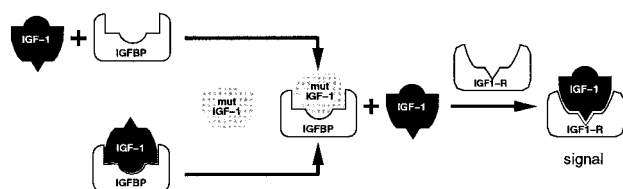


FIGURE 5: Schematic diagram of two mechanisms for indirect agonist activity. The interactions between IGF-1, the variant rh Y24L/Y31A IGF-1, IGF binding proteins (IGFBPs), and the type I IGF receptor (IGF1-R) are depicted in cartoon form. Although the IGF mutant is unable to bind to the receptor, it may produce IGF-like activity by either preventing newly synthesized IGFBP from binding to endogenous free IGF-1 (top) or displacing endogenous IGF-1 (following its dissociation) from IGFBP (bottom).

IGF-1 from its binding proteins. This occurs despite a paradoxical decrease in the total amount of circulating endogenous IGF-1 in the rat. In addition, the long-term effects in vivo of rh Y24L/Y31A IGF-1 suggest that tachyphylaxis may not reduce the effectiveness of a treatment involving IGF displacement from the binding proteins, provided that IGF-1 generation (for example, by stimulation of GH) is maintained. The results with diabetic rats also demonstrate for the first time that a liberation of endogenous IGF-1 from binding proteins can compensate for a reduction in insulin levels and lead to a maintained or reduced level of blood glucose. We have not tested the peptides in these rodent models because they do not inhibit the binding of IGF-1 to rat IGFBP-1 in vitro (data not shown). The peptides were selected for binding to human IGFBP-1, and it is perhaps not surprising that they show species specificity since they do show high specificity in inhibiting binding of IGF-1 to human IGFBP-1 but not human IGFBP-3 (Figure 1).

After this work was completed, work by Loddick et al. (18) was published showing that a similar variant of IGF-1 was neuroprotective in a rat model of brain damage, apparently acting by displacing IGF from its binding protein(s). Small molecules developed through molecular mimicry have the potential advantage of oral bioavailability, and perhaps greater accessibility to the central nervous system. The design of molecules specific for the individual binding proteins may also enhance the specificity of IGF-1 liberation, since different IGFBPs are produced at different target sites

within the body. The activity of indirect agonists will be limited by the amount of endogenous IGF-1 available for displacement. However, this could be a therapeutic advantage under circumstances in which a limited effect is desirable, as for instance in the case of an acute hypoglycemia induced by an oral agent. Ongoing studies will explore the utility of IGF mimics as indirect agonists in vivo.

## ACKNOWLEDGMENT

We thank J. Wells, B. Cunningham, and M. Dennis for advice and assistance with phage libraries, R. McDowell, W. Fairbrother, and M. Starovasnik for helpful discussions, the Genentech oligo synthesis and peptide purification groups, C. Quan and J. Burnier for assistance with peptide synthesis, D. Reifsnnyder for providing purified IGFBP-1 and IGFBP-3, P. Fielder for advice on IGFBPs, J. Liu for ultracentrifugation, and D. Yansura and R. Vandlen for producing mutant IGFs.

## SUPPORTING INFORMATION AVAILABLE

Details of the NMR structural analysis of peptide p1-01, chemical shifts and backbone coupling constants for the peptide (Table S1), and a summary of input to the peptide structure calculations and statistics of the resulting NMR ensemble (Table S2) (3 pages). Ordering information is given on any current masthead page.

## REFERENCES

- Barinaga, M. (1994) *Science* 264, 772–774.
- Bondy, C. A., Underwood, L. E., Clemmons, D. R., Guler, H.-P., Bach, M. A., and Skarulis, M. (1994) *Ann. Int. Med.* 120, 593–601.
- Clark, R. G., and Robinson, I. C. A. F. (1996) *Cytokine Growth Factor Rev.* 7, 65–80.
- Massagué, J., and Czech, M. P. (1982) *J. Biol. Chem.* 257, 5038–5045.
- Ullrich, A., Gray, A., Tam, A. W., Yang-Feng, T., Tsubokawa, M., Collins, C., Henzel, W., LeBon, T., Kathuria, S., Chen, E., Jacobs, S., Francke, U., Ramachandran, J., and Fujita-Yamaguchi, Y. (1986) *EMBO J.* 5, 2503–2512.
- De Meyts, P. (1994) *Diabetologia* 37 (Suppl. 2), S135–S148.
- Gill, R., Wallach, B., Verma, C., Ursø, B., DeWolf, E., Grötzinger, J., Murray-Rust, J., Pitts, J., Wollmer, A., De-Meyts, P., and Wood, S. (1996) *Protein Eng.* 9, 1011–1019.
- Jansson, M., Uhlen, M., and Nilsson, B. (1997) *Biochemistry* 36, 4108–4117.



9. Jones, J. I., and Clemmons, D. R. (1995) *Endocr. Rev.* 16, 3–34.
10. Bach, L. A., and Rechler, M. M. (1995) *Diabetes Rev.* 3, 38–61.
11. Baxter, R. C., and Martin, J. L. (1989) *Proc. Natl. Acad. Sci. U.S.A.* 86, 6898–6902.
12. Bagley, C. J., May, B. L., Szabo, L., McNamara, P. J., Ross, M., Francis, G. L., Ballard, F. J., and Wallace, J. C. (1989) *Biochem. J.* 259, 665–671.
13. Clemmons, D. R., Dehoff, M. L., Busby, W. H., Bayne, M. L., and Cascieri, M. A. (1992) *Endocrinology* 131, 890–895.
14. Oh, Y., Muller, M. L., Lee, D.-Y., Fielder, P. J., and Rosenfield, R. G. (1993) *Endocrinology* 132, 1337–1344.
15. Bayne, M. L., Applebaum, J., Underwood, D., Chicchi, G. G., Green, B. G., Hayes, N. S., and Cascieri, M. A. (1989) *J. Biol. Chem.* 264, 11004–11008.
16. Bayne, M. L., Applebaum, J., Chicci, G. G., Miller, R. E., and Cascieri, M. A. (1990) *J. Biol. Chem.* 265, 15648–15652.
17. Cascieri, M. A., and Bayne, M. L. (1994) in *Current Directions in Insulin-like Growth Factor Research* (LeRoith, D., and Raizada, M. K., Eds.) pp 33–40, Plenum Press, New York.
18. Loddick, S. A., Liu, X.-J., Lu, Z.-X., Liu, C., Behan, D. P., Chalmers, D. C., Foster, A. C., Vale, W. W., Ling, N., and De Souza, E. B. (1998) *Proc. Natl. Acad. Sci. U.S.A.* 95, 1894–1898.
19. Baserga, R. (1996) *Trends Biotechnol.* 14, 150–152.
20. Il'ichev, A. A., Minenkova, O. O., Tat'kov, S. I., Karpyshev, N. N., Eroshkin, A. M., Petrenko, V. A., and Sandakhchiev, L. S. (1989) *Dokl. Akad. Nauk SSSR* 307, 481–483.
21. Lowman, H. B., Bass, S. H., Simpson, N., and Wells, J. A. (1991) *Biochemistry* 30, 10832–10838.
22. Kunkel, T. A., Bebenek, K., and McClary, J. (1991) *Methods Enzymol.* 204, 125–139.
23. Bodanszky, M., and Bodanszky, A. (1984) in *The Practice of Peptide Synthesis*, Springer-Verlag, New York.
24. Grupe, A., Alleman, J., Goldfine, I. D., Sadick, M., and Stewart, T. A. (1995) *J. Biol. Chem.* 270, 22085–22088.
25. Cavanagh, J., Fairbrother, W. J., Palmer, A. G., and Skelton, N. J. (1995) in *Protein NMR Spectroscopy, Principles and Practice*, Academic Press, San Diego, CA.
26. Hwang, Q. N., and Shaka, A. J. (1995) *J. Magn. Reson.* 112A, 275.
27. Wüthrich, K. (1986) in *NMR of Proteins and Nucleic Acids*, John Wiley and Sons, New York.
28. Skelton, N. J., Garcia, K. C., Goeddel, D. V., Quan, C., and Burnier, J. P. (1994) *Biochemistry* 33, 13581–13592.
29. Havel, T. F. (1991) *Prog. Biophys. Mol. Biol.* 56, 43.
30. Charlton, H. M., Clark, R. G., Robinson, I. C. A. F., Goff, A. E. P., Cox, B. S., Bugnon, C., and Bloch, B. A. (1988) *J. Endocrinol.* 119, 51–58.
31. Scott, J. K., and Smith, G. P. (1990) *Science* 249, 386–390.
32. Lowman, H. B. (1997) *Annu. Rev. Biophys. Biomol. Struct.* 26, 401–424.
33. Geysen, H. M., Rodda, S. J., and Mason, T. J. (1986) *Mol. Immunol.* 23, 709–715.
34. O'Neil, K. T., Hoess, R. H., Jackson, S. A., Ramachandran, N. S., Mousa, S. A., and DeGrado, W. F. (1992) *Proteins* 14, 509–515.
35. Devlin, J. J., Panganiban, L. C., and Devlin, P. E. (1990) *Science* 249, 404–406.
36. Cwirla, S. E., Peters, E. A., Barrett, R. W., and Dower, W. J. (1990) *Proc. Natl. Acad. Sci. U.S.A.* 87, 6378–6381.
37. Greenwood, J., Willis, A. E., and Perham, R. N. (1991) *J. Mol. Biol.* 220, 820–827.
38. Felici, F., Castagnoli, L., Musacchio, A., Jappelli, R., and Cesareni, G. (1991) *J. Mol. Biol.* 222, 301–310.
39. Schultz, G. E., and Schirmer, R. H. (1979) in *Principles of Protein Structure* (Cantor, C. R., Ed.) pp 74–75, Springer-Verlag, New York.
40. Wrighton, N. C., Farrell, F. X., Chang, R., Kashyap, A. K., Barbone, F. P., Mulcahy, L. S., Johnson, D. L., Barrett, R. W., Jolliffe, L. K., and Dower, W. J. (1996) *Science* 273, 458–463.
41. Livnah, O., Stura, E. A., Johnson, D. L., Middleton, S. A., Mulcahy, L. S., Wrighton, N. J., Dower, W. J., Jolliffe, L. K., and Wilson, I. A. (1996) *Science* 273, 464–471.
42. Kay, B. K., Adey, N. B., He, Y.-S., Manfredi, J. P., Mataragnon, A. H., and Fowlkes, D. M. (1993) *Gene* 128, 59–65.
43. Martens, C. L., Cwirla, S. E., Lee, R. Y.-W., Whitehorn, E., Chen, E. Y.-F., Bakker, A., Martin, E. L., Wagstrom, C., Gopalan, P., Smith, C. W., Tate, E., Koller, K. J., Schatz, P. J., Dower, W. J., and Barrett, R. W. (1995) *J. Biol. Chem.* 270, 21129–21136.
44. Cooke, R. M., Harvey, T. S., and Campbell, I. D. (1991) *Biochemistry* 30, 5484–5491.
45. DeWolf, E., Gill, R., Geddes, S., Pitts, J., Wollmer, A., and Grotzinger, J. (1996) *Protein Sci.* 5, 2193–2202.
46. McDowell, R. S., Blackburn, B. K., Gadek, T. R., McGee, L. R., Rawson, T., Reynolds, M. E., Robarge, K. D., Somers, T. C., Thorsett, E. D., Tischler, M., Webb, R. R., II, and Venuti, M. C. (1994) *J. Am. Chem. Soc.* 116, 5069–5083.
47. Li, B., Tom, J. Y. K., Oare, D., Yen, R., Fairbrother, W. J., Wells, J. A., and Cunningham, B. C. (1995) *Science* 270, 1657–1660.
48. Braisted, A. C., and Wells, J. A. (1996) *Proc. Natl. Acad. Sci. U.S.A.* 93, 5688–5692.
49. Heding, A., Gill, R., Ogawa, Y., De Meyts, P., and Shymko, R. M. (1996) *J. Biol. Chem.* 271, 13948–13952.

BI980426E